

# Absolute and Convective Instabilities and Feedback Mechanisms

## Abstract:

Transition to turbulence and feedback mechanisms are a major area of focus for many fluid dynamitists. One way to look at this transition to turbulence is by looking at the instability regions that cause the flow to become turbulent. Absolute and convective instabilities are two types of instabilities, and within these categories are global and local instabilities, and linear, nonlinear, and slightly nonlinear flows. This paper will cover basic definitions of each of these types of instabilities, some of the governing equations, and finally some applications and case studies of each instability.

## Introduction:

Absolute and convective instabilities are important when studying mixing layers, jets, shear layers, and wakes of bluff bodies. The study of absolute and convective instabilities goes back as far as the 1950's when it was discovered that some wakes behind a bluff cylinder will have self-oscillatory motion [1]. All these flows will have some velocity gradient. Due to viscosity, this velocity gradient will attempt to come to equilibrium and cause the faster flow to transfer energy to the slower flow. This can cause instabilities to form, which in turn can cause instabilities to form and have detrimental effects on the performance of the vehicle or device. Whether this is an engine turbine blade, airplane wing, or even noise of an engine, these instabilities can have a large impact on the performance. Before building these structures, it is important to be able to accurately determine what will happen in the flow and thus design your model to be able to handle these conditions. In essence, studying these instabilities is crucial for flow control, initial aircraft design, and noise reduction as well as many other factors not discussed in this paper.

There are two main types of instabilities: local and global. These instabilities are relatively self-explanatory. Local instabilities are instabilities that occur in local velocity profiles. Examples of this would be regions just behind a bluff body, only regions upstream of the body, etc. Global instabilities are ones that cover the entire flow field. So, if a flow is globally unstable, a perturbation upstream would have the same effect as a perturbation downstream given time in the sense that the perturbation would grow the same over then entire flow field.

Within these types of instabilities are absolute and convective instabilities. Absolute instabilities are temporal. This means that they grow in time. So, in the laboratory frame of reference, a small perturbation would grow upstream and downstream. Another way to determine if the instability is absolute is to look at the front velocity of the upstream and downstream face of the wave packet caused by the initial perturbation. If the front velocities are moving in opposite directions, then the instability is absolute. Convective instabilities are spatial instabilities. These grow in space but dampen in time. A convective instability will grow as it gets swept downstream.

So, looking at the wave packet, the front velocity of the downstream side of the wave packet will be faster than the front velocity of the upstream side of the wave packet. Therefore, the wave packet will grow, but the initial x location of the perturbation will return to undisturbed conditions. Simply put, absolute instabilities propagate up and downstream and grow in time, whereas convective instabilities decay over time at the location of the perturbation, but are amplified as they move downstream.

Lastly, these flows can be linear, nonlinear, or weakly nonlinear. Linear instabilities have a “linear response to an initially localized impulse perturbation” [2]. These are based on linear stability theory and, if the flow is stable, will follow a Green’s function decay. These typically occur in flows with little freestream “noise” and are based on the assumption that perturbations are small. This is not the case for many real flows, so it provides a good starting point in modeling the flow, but it does not cover a wide range of flows. Nonlinear flows are more common, and these do not assume that the flow is parallel or small perturbations. These flows occur more often but are much harder to model as the math quickly becomes difficult by not making the parallel flow assumption. Finally, there are weakly nonlinear flows, also known as slightly nonlinear flows. These are again much harder to model than linear flows, but are more easily modeled than nonlinear flows. These flows occur more often than linear flows, and it is important to note that as the flow becomes weakly nonlinear, the linear model of the flow becomes invalid. This is why it is such a topic of interest to model weakly nonlinear flows as they are commonly occurring, but the linear model is not a good fit. The best example of a linear flow would be laminar flow over a flat plate. In real applications, low Reynold’s number flows over a wing are also typically modeled well by linear theory. Some nonlinear and slightly nonlinear examples are boundary layers, Poiseuille flow, separation bubbles, and other flows that are particularly chaotic or turbulent.

By looking at individual cases, it can be determined what the best way to model the flow will be, but this can be a very difficult task and it is often difficult to model the flow correctly. It is for these reasons why studying these instabilities has been a challenging problem for over 50 years.

### **Governing Equations:**

To begin, it is important to discuss Linear Stability Theory. To start, assume Navier Stokes and continuity with **Equations 1** and **2**.

$$\rho \left( \frac{\partial v_i}{\partial t} + u \frac{\partial v_i}{\partial x} + v \frac{\partial v_i}{\partial y} \right) = - \frac{\partial P}{\partial x} + \mu \left( \frac{\partial^2 v_i}{\partial x^2} + \frac{\partial^2 v_i}{\partial y^2} \right) \quad (1)$$

$$\frac{\partial u}{\partial x} + \frac{\partial v}{\partial y} = 0 \quad (2)$$

Next, we must decompose the flow into baseflow and small disturbances. Then we can plug these into **Equation 1** and assume small perturbations. We note here that the first assumption we make

about the flow is that the perturbations are small. This is important as in many real flows the perturbations are not small according to the definition of this assumption.

$$u = U + u' \quad (3)$$

$$\begin{aligned} \rho \left( \frac{\partial}{\partial t} (U + u') + u \frac{\partial}{\partial x} (U + u') + v \frac{\partial}{\partial y} (U + u') \right) = \\ = - \frac{\partial}{\partial x} (P + p') + \mu \left( \frac{\partial^2}{\partial x^2} (U + u') + \frac{\partial^2}{\partial y^2} (U + u') \right) \end{aligned} \quad (4)$$

$$U(x, y) = U(y) \quad (5)$$

The next important assumption made is to assume the baseflow is parallel. From this and continuity, we get **Equation 6**.

$$\frac{\partial P}{\partial x} = \mu \frac{\partial^2 u}{\partial y^2} \quad (6)$$

$$\psi'(x, y, t) = \phi(y) e^{i(\alpha x - \omega t)} \quad (7)$$

Lastly, we assume disturbances are in the form of traveling waves. In this equation, if  $\alpha$  is real and  $\omega$  is complex, the traveling wave assumption is a temporal case. In this case, the function would model an absolute instability. On the contrary, if  $\alpha$  is complex and  $\omega$  is real, the function would model a spatial case and thus model a convective instability. This means that when modeling flows, it is important to know what assumption to make in the traveling wave assumption to best capture where in the flow each instability would occur.

$$i \frac{\partial \psi}{\partial t} = \left( \omega_0(X) + \frac{1}{2} \omega_{kk}(X) k_0(X)^2 \right) \psi + i \omega_{kk}(X) k_0(X) \frac{\partial \psi}{\partial x} - \frac{1}{2} \omega_{kk}(X) \frac{\partial^2 \psi}{\partial x^2} + \gamma(X) |\psi|^2 \psi \quad (8)$$

$$\left( \frac{\partial}{\partial t} + U(y, X) \frac{\partial}{\partial x} \right) \Delta \psi - \frac{\partial^2 U}{\partial y^2}(y, X) \frac{\partial \psi}{\partial x} + \left( \frac{\partial \psi}{\partial y} \frac{\partial}{\partial x} - \frac{\partial \psi}{\partial x} \frac{\partial}{\partial y} \right) = \frac{1}{Re} \Delta^2 \psi \quad (9)$$

$$\omega = \Omega^l(k, X) \quad (10)$$

$$\omega = \Omega^{nl}(k, X) \quad (11)$$

The next important equation to discuss is the Ginzburg-Landau equation. The inhomogeneous Ginzburg-Landau evolution equation for a complex field is written in **Equation 8**. By inserting the stream function just as in the Linear Stability Theory, **Equation 9** can be derived. This equation is a function of the inlet velocity profile and the pressure distribution of the flow along the x axis, making it ideal for numerically modeling the entire flow field with a synthetic wake that does not require an obstacle to generate the wake. Lastly, the goal is to solve for frequencies in the flow which are shown in **Equations 10** and **11**, where **10** is the linear solution and **11** is the nonlinear solution. This shows that flows can be modeled for both the linear and nonlinear solutions, but solving each will require different steps. The linear solution often times makes assumptions that will simplify the problem, but ignore parts of the flow that could have a large impact on the results.

For the linearized Ginzburg-Landau case, and impulse response modeled as a Green's function can be introduced, and the result of this can show whether the flow is stable, absolutely, or convectively unstable. The relations are as follows [3].

1. The basic flow is **linearly stable** if the  $\lim_{t \rightarrow \infty} G(x, t) = 0$  along all rays  $x/t = \text{const}$
2. Flow is **linearly unstable** if  $\lim_{t \rightarrow \infty} G(x, t) = \infty$  along at least one ray  $x/t = \text{const}$
3. Flow is **convectively unstable** if  $\lim_{t \rightarrow \infty} G(x, t) = 0$  along the ray  $x/t = 0$
4. Flow is **absolutely unstable** if the  $\lim_{t \rightarrow \infty} G(x, t) = \infty$  along the ray  $x/t = 0$

Finally, looking at weakly nonlinear cases, a WKBJ analysis is typically done. The basic function in all WKBJ analyses is a slow streamwise variable where epsilon is the criticality parameter and x is the streamwise location. This paper will follow the derivation by Dizes, Huerre, Chomaz, and Monkewitz [4].

$$X = \epsilon x \quad (12)$$

The weakly nonlinear case begins with the nonlinear Ginzburg-Landau equation (**equation 13**) where all coefficients are assumed to be complex, continuous, and functions of some control parameter R. Close to the linear region of the flow, the Landau equation is a good approximation of the flow. Then, the determining factor in the bifurcation of the flow is the real part of the Landau equation. The important assumption this makes is that it is derived from a small parameter  $(R - R_c)$ , and if the criticality parameter is greater than zero the expression takes the form of **equation 15**. Without going into too much detail, the constants in this equation are similar to the linear equation. This shows the relation to the linear equation, but still holds true from some flows past the linear flow regime.

$$\left[ i \frac{\partial}{\partial t} + \frac{\omega_{kk}}{2} \frac{\partial^2}{\partial x^2} - i \omega_{kk} (k_s + k_{0X}(X - X_s)) \frac{\partial}{\partial x} - \left( \frac{\omega_{kk}}{2} (k_s + k_{0X}(X - X_s))^2 + \left( \omega_s + \frac{\omega_{0XX}}{2} (X - X_s)^2 \right) \right) \right] \psi = c |\psi|^2 \psi \quad (13)$$

$$\frac{\partial A}{\partial t} = -i \omega_{g0}(\varepsilon, R) A + L(\varepsilon, R) |A|^2 A \quad (14)$$

$$L(\varepsilon, R_c) = c K e \frac{\Theta}{\varepsilon} \quad (15)$$

### Differences of Absolute and Convective Instabilities:

**Figure 1** is taken from a paper by Huerre and Mokewitz [3] and shows how each type of instability behaves. In this figure, “R” is a criticality term that could represent Reynold’s number, frequency, or any other term studied for a particular case. The flow starts as linearly stable (**1a**), then becomes linearly convectively unstable (**1b**), and finally linearly absolutely unstable (**1c**) as this R term is increased. The easiest example to relate this to is Reynold’s number. According to these charts, once Reynold’s number is increased to a critical value, the region transitions to convectively unstable. As the Reynold’s number is further increased to a bifurcation factor, the flow again transitions to absolutely unstable.

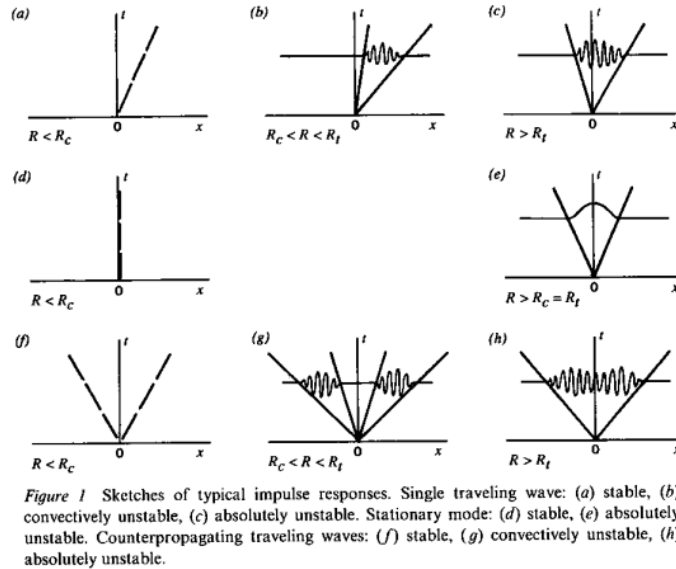


**Figure 1 – schematic of linearly stable, absolute, and convective instabilities [3].**

While each type of instability has different characteristics, they are also formed from different flow characteristics. For both instabilities, velocity gradients drive the instability. In fact,

an inflection point in the velocity profile is a necessary condition of convective or absolute instabilities, even though it is not a sufficient condition of either. For any case, convectively unstable flows generally have a smaller velocity gradient than the absolutely unstable regions. In the case of reverse flow, convective instabilities will generally have a reverse flow of less than 15 percent. However, this is just a rule of thumb, and a questionable one at that, as reverse flow of as low as 7 percent in a three-dimensional laminar separation bubble was seen to cause flow to become absolutely unstable [5]. Alternatively, absolutely unstable flows occur in regions of higher velocity gradients. Thus, in reverse flow, absolutely unstable regions usually occur around 15 percent reverse flow and higher (again, just an approximation). So, absolutely unstable regions are more likely to occur in areas such as just behind a bluff body, around jets of air, and at the exit of stationary jet engines, while convectively unstable regions are more likely to occur far from the blunt body and around jet engines that are actually in flight. Each of these can be observed and are based on the velocity gradient having an inflection point.

Another common problem studied is forcing. From a flow control standpoint, this is a very important topic. As noted before, convective instabilities amplify downstream, but the flow will eventually return to its unperturbed state. However, if the flow is forced constantly at certain frequencies, then these amplifications will begin to dominate far from the initial forcing location [6]. For relatively small inputs, the wave packet grows very large downstream, and thus the signal to noise ratio for convective instabilities theoretically approaches infinity for small perturbations. This shows that convective instabilities are very susceptible to forcing, and regions that are convectively unstable must be either protected from this forcing or utilized to force the flow to trip to turbulent (this will be discussed further in the application section). Contrary to this, absolute instabilities will theoretically have a signal to noise ratio of zero. For these regions, a small perturbation will cause the entire flow field to become noisy, and everything will be enveloped by this instability. This means that an input perturbation no longer has an impact like in the convectively unstable region, which causes forcing to have little effect in these regions [7].

It is then important to discuss nonlinear effects. The first condition is that in order for there to be a nonlinear global mode, there must first exist an absolutely unstable region [8]. While there still can exist a nonlinearly unstable local region in the absence of an absolutely unstable region, there cannot exist a nonlinear global mode. It is very important to determine when a region becomes nonlinear because even when the flow becomes slightly nonlinear, these linear predictions of instabilities have large error. However, by finding a region of absolute instability, a global absolutely unstable region is possible but not certain.

A figure comparing linear and nonlinear instabilities is shown below in **figure 2**. As shown, the linear graphs have smooth wave fronts that asymptotically relax for all cases: stable and unstable. Contrarily, the nonlinear cases have sharp wave fronts. This drastic change in flow conditions no longer satisfies the parallel flow assumption as the perturbations and change in flow now affects the mean flow profile. Although linear and nonlinear are two separate problems, this does not mean they do not show up in the same flow fields. In fact, they are likely tied together in that linear regions turn into nonlinear regions. An example of this is in **figure 4** which depicts a laminar separation bubble. Near the front of the bubble, the velocity gradient is smaller (this is the

region of convective instability) and the perturbations are still not large, but as the flow moves further downstream the perturbations become larger. In this region, the linear assumptions no longer hold true, and the nonlinear effects must be accounted for in modeling the flow.

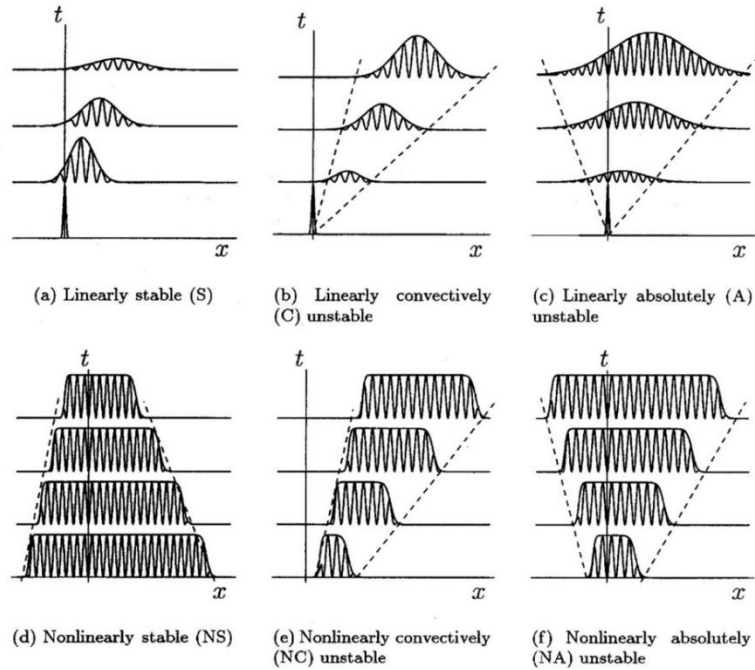


**Figure 2 – comparison of linear and nonlinear perturbations [2].**

In **figure 3**, three different graphs are shown: linear global mode, nonlinear “hat” mode, and nonlinear “elephant” mode. It can be seen that the wave fronts of the hat mode and the elephant modes both do not asymptotically decay as in the linear mode. This further emphasizes that the shape of the wave packet for nonlinear modes is clearly sharper for real cases. As a note, hat modes have not been found experimentally. These modes have only been seen on rare occasions, and it is theorized that these modes do not occur in real situations very often if at all. It is also worth noting the grey region in **figure 3** for each graph. As will be discussed later, this is the absolutely unstable region and is important for causing those nonlinear global modes.

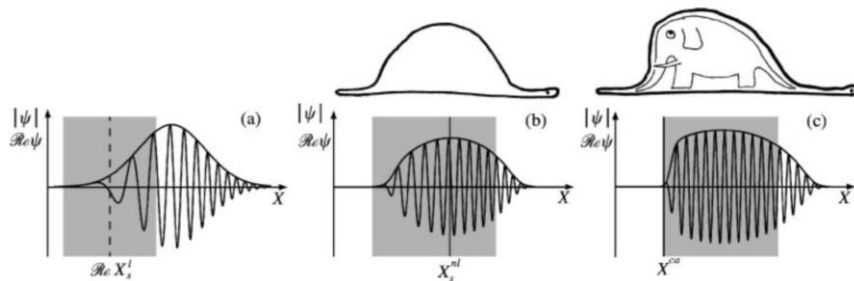


Figure 1. Shapes of CGL global modes. Shaded regions indicate extent of AU domain. (a) Linear global mode. (b) Nonlinear soft global mode or hat mode. (c) Nonlinear steep global mode or elephant mode. The names “hat” and “elephant” have been chosen in reference to Saint-Exupéry (1946).

**Figure 3 – Types of nonlinear modes [8].**

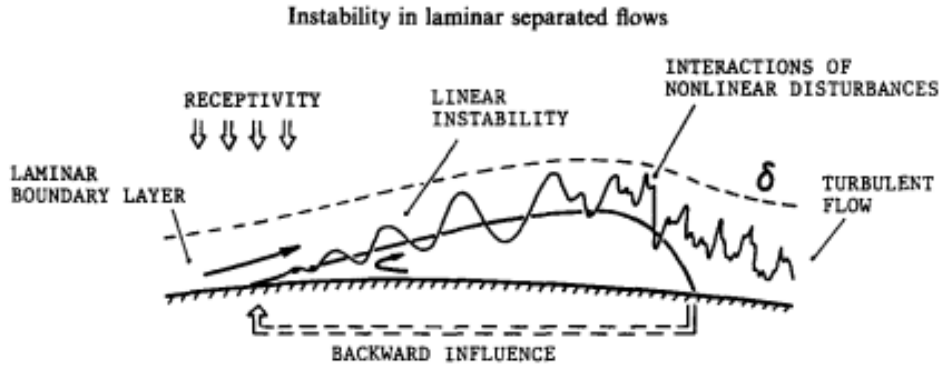


FIG. 1. Instability and transition to turbulence in a laminar separation bubble.

**Figure 4 – Instability regions in a laminar separation bubble [6].**

The final point to note is that regions can share instability mechanisms. For example, a flow could be linearly absolutely unstable and nonlinearly convectively unstable in the same region. This is partially due to three dimensional effects. As an example, in crossflow it is still unclear in most cases whether the dominate instability is due to the streamwise or the spanwise instability. While it can be shown that they both exist, it is much harder to prove which one has more of an influence on the flow. Shown in **figure 5** is a chart that depicts a case where the flow is nonlinearly absolutely unstable, nonlinearly globally unstable, and linearly absolutely unstable all in the same region.

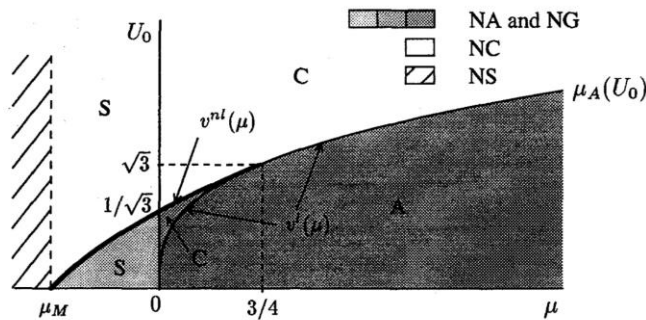


Fig. 3. Nonlinearly absolutely (NA) unstable domain (shaded regions) in parameter space. The dark gray region represents the linearly absolutely (A) unstable region which is totally embedded in the NA region. The system is NA unstable in the medium and light gray regions whereas it is linearly convectively unstable (C) or linearly stable (S). The system is nonlinearly convectively (NC) unstable in the white region. The nonlinearly stable (NS) region ( $\mu < \mu_M$  where  $\mu_M = -3/16$  is the Maxwell point) is totally embedded in the linearly stable (S) region. Section 3 will show that an NG mode exists in the three shaded regions.

**Figure 5 – regions of instabilities [2].**

**Applications and Case Studies:**

With all this said, it can be estimated where each region will appear and what effect it will have on the flow. For example, many studies have been done with cylinders and the wakes behind these cylinders. It has been shown several times that the region just behind the bluff body is dominated by absolute instabilities, whereas the region far behind the wake is dominated by



convective instabilities. A numerical study by Monkewitz and Nguyen [6], another by Huerre and Monkewitz [7], and a final study by Pier and Huerre [8] was conducted on the wake of a 2D bluff body. By using **equation 16** with  $N$  as the term that varies the  $x$  location of the data, they were able to determine the resulting instabilities along the streamwise direction of the flow in relation to the bluff body. Shown in **figure 6**, they found the critical value of  $\omega$  that switched the instability mechanism from convective to absolute. In relation to the figure, when the imaginary value of  $\omega$  switches from negative to positive values, the instability mechanism switches from convective to absolute. So, in this figure, the noted points along the line are different velocity ratios along the mixing layer. Thus, they concluded that a mixing layer velocity ratio of 1.315 was the bifurcation value at which the absolutely unstable region begins. In these studies, they found that just behind the bluff body is a region of absolute instability. Looking back to **figure 3**, this is an important property because the grey region of the flow is the region of absolute instability. This shows that the absolutely unstable region causes these limit cycles behind the body. Limit cycles, in this case, are self-sustaining oscillations in the wake behind the bluff body. This means that due to the absolutely unstable region behind the body, these oscillations are nearly unavoidable without adding some geometry to the flow (assuming the other critical parameters like Reynold's number are kept the same). An example of some geometry to add would be a flat splitter plate behind the body. This could reduce the mixing layer velocity ratio in the wake and in turn remove the absolutely unstable region behind the flow. This principle works in favor of airfoils because the blunt leading edge is extended and brings the two sides of the flow together like a splitter plate.

$$F(y) = [1 + \sinh^{2N}(y \sinh^{-1} 1)]^{-1} \quad (16)$$

After this region of absolute instability, the flow changes back to convectively unstable, and this is why the eddies grow so rapidly after the absolutely unstable region. This is from the fact that the far field is dominated by the convectively unstable region. The last chart that shows this is **figure 8**. This compares the  $x$  location behind a wake with the Reynold's number of the flow. In this graph,  $S$  is defined as the density of the wake over the density of the freestream. This means that an  $S$  value of one would be just behind the body in the wake, and an  $S$  value of zero would be far from the body. As shown, even at lower  $Re$  values, the region just behind the body is almost always absolutely unstable. Conversely, the region far from the body is almost always convectively unstable, even at higher  $Re$  values which would raise the mixing layer velocity ratio.

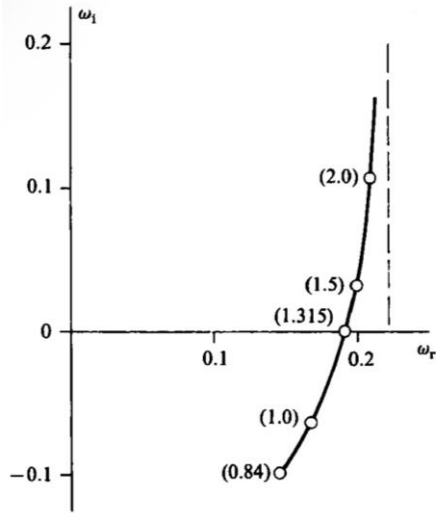


Figure 6 – velocity ratio of a mixing layer for transition to absolute instabilities [7].

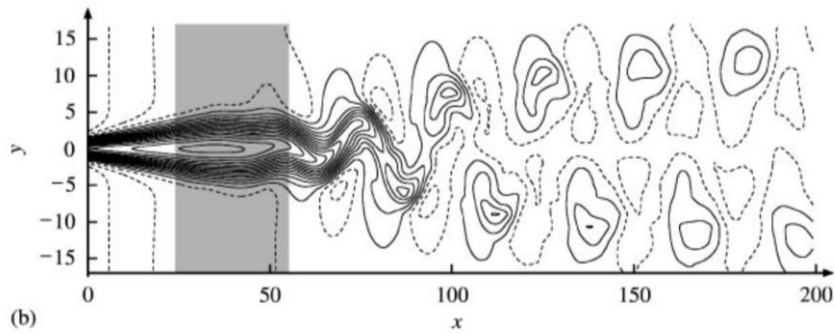


Figure 7 – instability region behind a bluff body [8]

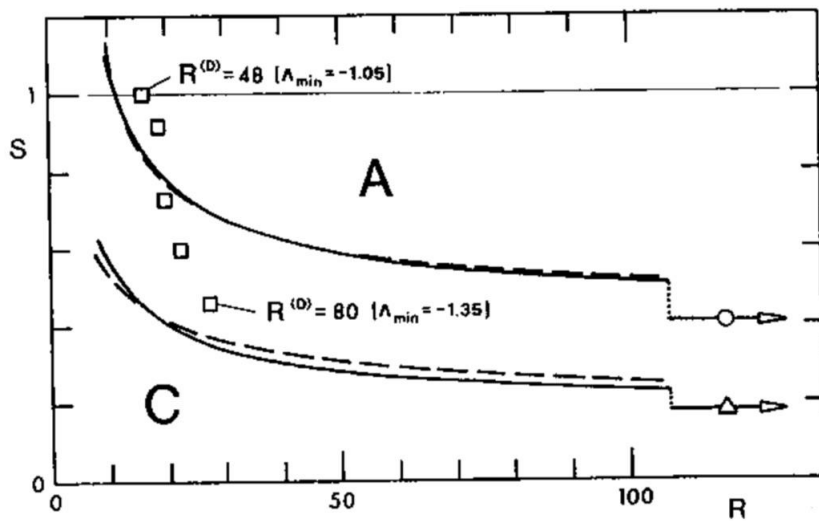
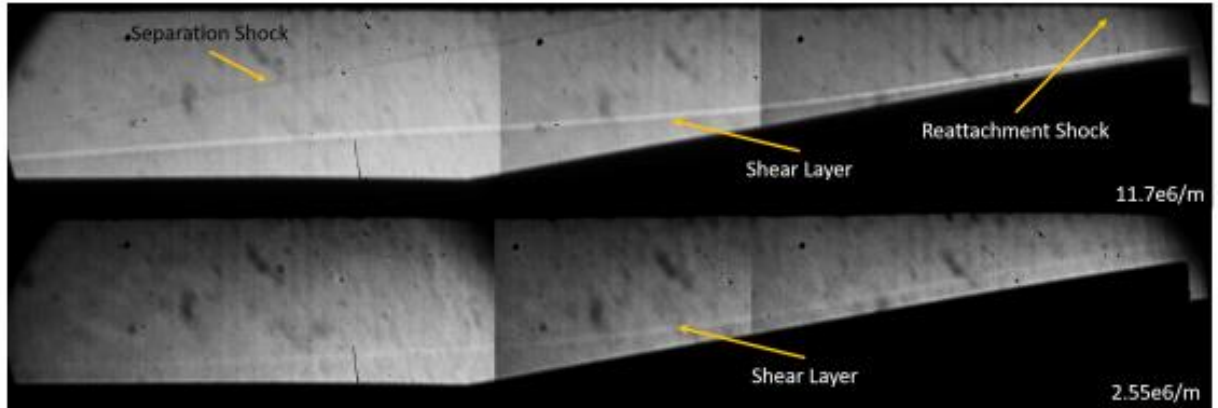


Figure 8 – Absolute and convectively unstable regions behind a bluff body [6]

Some applications of these principles are mostly related to flow control. It is very important to be able to not only predict the flow, but know how to control the flow as well. In cases of an airfoil, particularly for low-speed vehicles, if the flow separates and forms a large separation region, that entire section is no longer producing lift which could be detrimental to the vehicle and will certainly be harmful to the performance of the vehicle at least. By knowing that a region is convectively unstable, one method being tested is tripping the flow with essentially small steps on the surface, and also forcing the flow with a ribbon. As mentioned previously, convectively unstable regions have a very high signal to noise ratio, and if the ribbon is vibrated at the correct frequency, the flow can be sufficiently disturbed to create a mixing layer and prevent the flow from becoming unattached [12].

Another application can be to reduce the noise produced by a jet. Monkewitz and Sohn [9] discovered that much of the noise of a jet engine came from wave packets. As a result, by forcing the flow in the convectively unstable region, this noise can be significantly reduced. Another important find that Monkewitz and Sohn discussed was that in testing for these instabilities in jet engines, it is important to note that the tests are done on a test stand. This means no flow will be moving around the engine. This is important because it means that the mixing layer ratio of the velocities is very high around the jet, and thus the region would be absolutely unstable. However, in flight, the air around the engine is moving, and this causes the velocity ratio to be much smaller and the flow can become convectively unstable rather than absolutely.

For high-speed flows, Benitez [10] discovered that different instabilities could occur with the same conditions based only on parameters like angle of attack or even just freestream noise. **Figure 9** shows an experiment done where angle of attack was varied to see its effects on the flow. Interestingly, she found that adding an angle of attack made the instabilities switch from convective to absolute in the separation bubble after the flare. She also ran a study to look at the effect freestream noise had on the flow. Looking at **figure 10**, the coherence of zero indicates an absolute instability, whereas a coherence of one indicates a convective instability. This comparison shows there is a clear rise in the 50-100 kHz frequencies, indicating a change from absolute to convective instabilities in the presence of freestream noise. It is not clear why this happens, but one explanation is that the noisy flow would have a fuller boundary layer profile, and thus reverse flow would be worse in the quiet flow. This would cause the instability to switch from convective to absolute as the shear layer velocity gradient becomes stronger.



**Figure 9 – Effect of angle of attack on instabilities [10].**

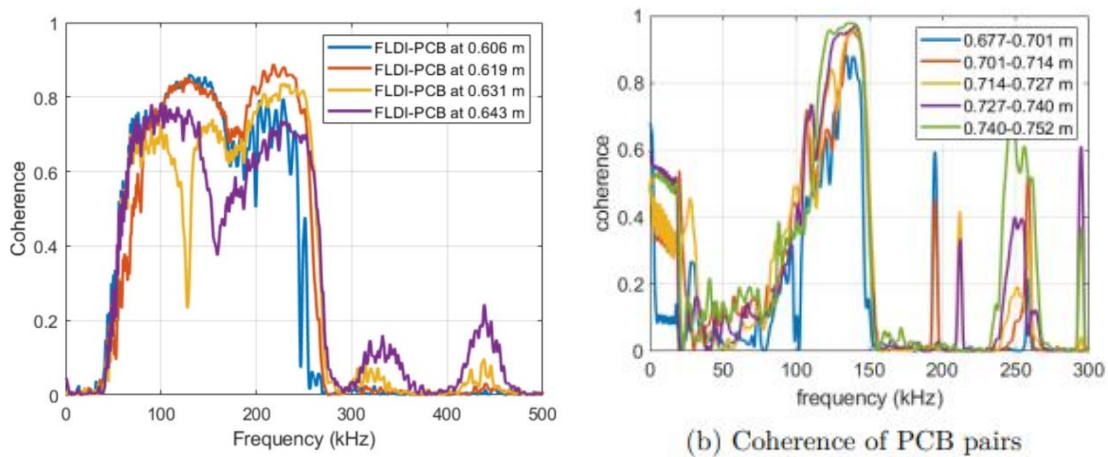


**Figure 10 – Coherence of instabilities in freestream noise and quiet flow [10].**

### Conclusion:

In conclusion, there are two types of instabilities: absolute and convective. In these, there are linear, nonlinear, slightly nonlinear, global, and local. These instabilities are important to study for mixing layers, shear flow, jets, and wakes. In each of these flows, absolute instabilities will grow upstream and downstream and eventually dominate the flow field. Convectively unstable regions will get swept downstream, and the flow will eventually return to the undisturbed state, but they grow in the streamwise direction. In modeling these flows, it is a very case by case basis. While some overarching themes are common for all cases, it is very difficult to predict what will happen in the flow. For linear instability regions this can be done relatively easily, but this region is often small and nonlinear effects take over rapidly. For slightly nonlinear flows, these can also be modeled better than the fully nonlinear region, but similarly to the linear region, it is often small and the results can diverge quickly from the true answers due to the assumptions of linear and nearly linear flow and small perturbations.

## References

1. C. W. Rowley, T. Colonius, and A. J. Basu, "On self-sustained oscillations in two-dimensional compressible flow over rectangular cavities," *Journal of Fluid Mechanics*, vol. 455, pp. 315–346, Mar. 2002, doi: 10.1017/s0022112001007534
2. Couairon, A., and Chomaz, J., "Absolute and Convective Instabilities, Front Velocities and Global Modes in Nonlinear Systems," *Physica D: Nonlinear Phenomena*, Vol. 108, No. 3, 1997, pp. 236–276. [https://doi.org/10.1016/s0167-2789\(97\)00045-6](https://doi.org/10.1016/s0167-2789(97)00045-6)
3. Huerre, P., and Monkewitz, P. A., "Local and global instabilities in spatially developing flows," *Annual Review of Fluid Mechanics*, vol. 22, 1990, pp. 473–537.
4. S. L. Dizès, P. Huerre, J. Chomaz, and P. A. Monkewitz, "Nonlinear Stability Analysis of Slowly-Diverging Flows: Limitations of the Weakly Nonlinear Approach," in *Springer eBooks*, 1993, pp. 147–152. doi: 10.1007/978-3-662-00414-2\_34.
5. D. Borgmann, "Investigation of active control of boundary layer transition in laminar separation bubbles," Ph.D. dissertation, University of Arizona, 2023.
6. P. A. Monkewitz and L. Nguyen, "Absolute instability in the near-wake of two-dimensional bluff bodies," *Journal of Fluids and Structures*, vol. 1, no. 2, pp. 165–184, Apr. 1987, doi: 10.1016/s0889-9746(87)90323-9
7. P. Huerre and P. A. Monkewitz, "Absolute and convective instabilities in free shear layers," *Journal of Fluid Mechanics*, vol. 159, no. 1, p. 151, Oct. 1985, doi: 10.1017/s0022112085003147
8. Pier, B., and Huerre, P., "NONLINEAR SYNCHRONIZATION IN OPEN FLOWS," *Journal of Fluids and Structures*, Vol. 15, Nos. 3–4, 2001, pp. 471–480. <https://doi.org/10.1006/jfls.2000.0349>
9. P. A. Monkewitz and K. D. Sohn, "Absolute instability in hot jets and their control," AIAA, Jul. 1986, doi: 10.2514/6.1986-1882
10. Benitez, E. K., "Instability Measurements on Two Cone-Cylinder-Flares at Mach-6," dissertation, 2021.
11. Chomaz, J., "Absolute and Convective Instabilities in Nonlinear Systems," *Physical Review Letters*, Vol. 69, No. 13, 1992, pp. 1931–1934. <https://doi.org/10.1103/physrevlett.69.1931>
12. W. Koch, "Local instability characteristics and frequency determination of self-excited wake flows," *Journal of Sound and Vibration*, vol. 99, no. 1, pp. 53–83, Mar. 1985, doi: 10.1016/0022-460x(85)90445-6
13. L. Jones, R. D. Sandberg, and N. D. Sandham, "Stability and receptivity characteristics of a laminar separation bubble on an aerofoil," *Journal of Fluid Mechanics*, vol. 648, pp. 257–296, Apr. 2010, doi: 10.1017/s0022112009993089.
14. Y. Hwang and H. G. Choi, "Sensitivity of global instability of spatially developing flow in weakly and fully nonlinear regimes," *Physics of Fluids*, vol. 20, no. 7, Jul. 2008, doi: 10.1063/1.2952010.

15. L. Brandt, D. S. Henningson, and D. Ponziani, "Weakly nonlinear analysis of boundary layer receptivity to free-stream disturbances," *Physics of Fluids*, vol. 14, no. 4, pp. 1426–1441, Apr. 2002, doi: 10.1063/1.1456062.
16. P. A. Monkewitz, P. Huerre, and J. Chomaz, "Global linear stability analysis of weakly non-parallel shear flows," *Journal of Fluid Mechanics*, vol. 251, pp. 1–20, Jun. 1993, doi: 10.1017/s0022112093003313.